Zoosyst. Evol. 101 (4) 2025, 1799–1813 | DOI 10.3897/zse.101.161907

PENSOFT

für Naturkunde MUSEUM FÜR NATURKUNDE BERLIN

One more new ring nematode of the *Xenocriconemella macrodora* species-complex (Nematoda, Criconematidae): *Xenocriconemella persica* sp. nov. from Iran

Mohsen Asgari[1], Somayeh Mokhtari[1], Ali Eskandari[1], Carolina Cantalapiedra-Navarrete[2], Inmaculada Criado-Navarro[2], Juan E. Palomares-Rius[2], Pablo Castillo[2], Antonio Archidona-Yuste[2]

1 *Department of Plant Protection, Faculty of Agriculture, University of Zanjan, 45371-38791 Zanjan, Iran*

2 *Department of Crop Protection, Institute for Sustainable Agriculture, Avenida Menéndez Pidal s/n, 1Campus de Excelencia Internacional Agroalimentario, ceiA3, 4004 Córdoba, Spain*

https://zoobank.org/7A64BDE0-60EE-4402-A0A7-7DA43CC72D14

Corresponding author: Antonio Archidona-Yuste (antonio.archidona@ias.csic.es)

Academic editor: A. Schmidt-Rhaesa ♦ **Received** 12 June 2025 ♦ **Accepted** 18 August 2025 ♦ **Published** 17 September 2025

Abstract

Despite the identification of several species within the *Xenocriconemella macrodora* species complex in recent years, it is likely that even greater species diversity exists within this group. In the present study, a population of ring nematodes was collected from forested regions in northern Iran, exhibiting a high degree of morphological similarity to *X. macrodora* and related taxa. Morphological, morphometric, and molecular analyses, conducted using an integrative taxonomic approach, confirmed the presence of a novel species: *Xenocriconemella persica* **sp. nov.** Only females were observed, suggesting parthenogenetic reproduction. The species is characterised by a bare body measuring 234–316 µm in length. The lip region comprises two annuli that are continuous with the body contour, with the second annulus enclosed by the first. The stylet is slender and flexible, measuring 83–103 µm, and constitutes 28.4–37.0% of the total body length. The excretory pore is situated 1–9 annuli anterior to the stylet knobs, at a distance of 83–100 µm from the lip region. The female reproductive system is monodelphic and prodelphic, occupying 30.2–46.1% of the body length, with the vagina slightly curved ventrally. The anus is located 6–9 annuli from the tail terminus, and the tail is short, conoid, and bluntly rounded. Ribosomal and mitochondrial markers (D2-D3 expansion domains of 28S, ITS, partial 18S rRNA, and COI), together with phylogenetic analyses, revealed that this species occupies a distinct evolutionary position relative to other members of the *X. macrodora* complex. The findings indicate the presence of a cryptic species within this group, which, despite morphological resemblance, exhibits clear genetic divergence from closely related taxa. This study contributes to our understanding of hidden diversity in morphostatic taxa and underscores the significance of molecular data in species delimitation.

Key Words

COI, cryptic species, D2-D3, integrative taxonomy, ITS, 18S rRNA, morphometry

Introduction

The genus *Xenocriconemella* De Grisse & Loof, 1965 comprises small ectoparasitic nematodes characterised by a heavily annulated cuticle and a relatively long stylet, which typically occupies approximately 40% of the total body length. For decades, *X. macrodora* (Taylor 1936) De Grisse and Loof 1965 was the only widely accepted species within the genus, owing to its stable morphology, broad range of stylet lengths, and the limited number of studies addressing its molecular diversity. However, recent integrative taxonomic efforts, particularly in the Iberian Peninsula and Central America, have challenged this view, revealing a cryptic species complex and leading to the description of several new taxa, including *X. iberica* Archidona-Yuste et al., 2024, *X. paraiberica* Archidona-Yuste

Copyright *Asgari, M. et al.* This is an open access article distributed under the terms of the Creative Commons Attribution License (CC BY 4.0), which permits unrestricted use, distribution, and reproduction in any medium, provided the original author and source are credited.

et al., 2024, *X. pradense* Archidona-Yuste et al., 2024, *X. costaricense* Peraza-Padilla et al., 2024, *X. andreae* Cantalapiedra-Navarrete et al., 2024, and *X. tica* Peraza-Padilla et al., 2025. These discoveries underscore the underestimated biodiversity within the genus and highlight the importance of molecular markers in resolving taxonomic ambiguities in morphologically conserved taxa.

Such findings have not only expanded the species inventory of *Xenocriconemella* but also emphasised the value of combining morphological, morphometric, and molecular approaches to delimit species boundaries, particularly in groups prone to cryptic speciation. Molecular divergence without clear morphological differentiation is common among plant-parasitic taxa, as demonstrated in previous studies (Cantalapiedra-Navarrete et al. 2013; Archidona-Yuste et al. 2016, 2020; Cai et al. 2020; Clavero-Camacho et al. 2021). Consequently, integrative taxonomy has become essential for detecting and describing hidden diversity (Proudlove and Wood 2003; Dayrat 2005; Fišer and Koselj 2022).

In Iran, the genus *Xenocriconemella* was first reported by Eskandari et al. (2006) and Eskandari (2018) under the name *X. macrodora*, isolated from soil samples around the roots of alder (*Alnus subcordata* C.A. Meyer) in the Olang Forest near Shahrud County, in the northeast of the country. Although molecular markers were not employed in that study, the findings confirmed the presence of *Xenocriconemella* in Iranian forest ecosystems and highlighted the need for further integrative research to clarify its taxonomy and diversity. Subsequent studies by Ghaderi et al. (2012) documented its occurrence in oak (*Quercus* sp.) forests in Gilan Province, northern Iran, followed by Niasti et al. (2016), who recorded its presence in association with other forest trees in the same region. More recently, Zaker Abbasali et al. (2024) confirmed its presence in the rhizosphere of walnut trees (*Juglans* sp.) in the Jovarem forests of Mazandaran Province, further supporting its distribution across the northern woodlands of Iran. However, all previously reported populations were identified solely on the basis of morphological features, without supporting molecular data, leaving species delimitation unresolved. The discovery and integrative characterisation of an unidentified *Xenocriconemella* population in the present study represents a significant advancement in resolving the taxonomic complexity of this genus in Iran.

Previous research has demonstrated that morphological variation within *Xenocriconemella* is often insufficient for species delimitation due to the presence of cryptic species complexes, rendering molecular approaches indispensable for accurate identification. Ribosomal and mitochondrial DNA markers, including the D2–D3 expansion domains of 28S rRNA, ITS, 18S rRNA, and cytochrome c oxidase subunit I (COI), have been widely employed to resolve taxonomic ambiguities and infer phylogenetic relationships within Criconematidae, further supporting the validity and monophyly of *Xenocriconemella* (Clavero-Camacho et al. 2021; Nguyen et al. 2022; Archidona-Yuste et al. 2023, 2024). The transition from morphological to integrative taxonomy in *Xenocriconemella* has revealed a compelling model for cryptic speciation (Archidona-Yuste et al. 2024; Peraza-Padilla et al. 2025).

In this study, we aimed to: (i) investigate the morphological, morphometric, and molecular characteristics, specifically ribosomal (D2-D3 expansion domains of 28S rRNA, ITS region, partial 18S rRNA) and COI markers, of an unidentified *Xenocriconemella* population collected from a natural habitat in Iran and compare it with other species in the *X. macrodora*-species complex; and (ii) elucidate the phylogenetic relationships of this unidentified *Xenocriconemella* population within the *X. macrodora*-species complex. This research addresses a significant gap in our understanding of nematode biodiversity in Iran and contributes to a broader comprehension of the genus *Xenocriconemella* at a global scale.

Material and methods

Nematode isolation and morphometrical characterization

Nematode surveys conducted in winter 2024 in Iran aimed to decipher the molecular and morphological diversity of *Xenocriconemella* species in the natural forests of northern Iran, leading to the detection of an unidentified *Xenocriconemella* species. Soil samples were collected from the rhizosphere soil of forest trees (*Alnus glutinosa* (L.) Gaertn., and *Fagus orientalis* Lipsky) in Gilan province, North Iran, at depths ranging from 5 to 40 cm. The nematodes were extracted using the rapid flotation-sieving and centrifugation method (Jenkins 1964), then killed and fixed by hot FPG solution (4:1:1 formaldehyde: propionic acid: glycerine), processed to anhydrous glycerine (De Grisse 1969), and mounted on permanent slides in glycerine using paraffin wax.

Microscope slides were prepared to enable morphological and morphometric analysis, which was conducted using a light microscope equipped with a Dino-eye microscope eyepiece camera in conjunction with its Dino Capture version 2.0 software. Materials and methods used for light microscopy (LM) and morphometric studies followed the same protocols outlined by Archidona-Yuste et al. (2024) and other researchers (Seinhorst 1966; De Grisse 1969). The following abbreviations (i.e. measurements and ratios) are used in the morphological descriptions, data analyses and figures: **L**, (total body length); **a** = body length/maximal body width; **b** = body length/pharyngeal length; **c** = body length/tail length; **c'** = tail length/body width at anus; **O** = distance between stylet base and orifice of dorsal pharyngeal gland as percentage of stylet length; **R** = total number of body annuli; **Roes** = number of annuli in pharyngeal region; **Rex** = number of annuli between anterior end of body and excretory pore; **Rst** = number of body annuli between labial disc and stylet knobs; **RV** = number of annuli between posterior end

of body and vulva; **Rvan** = number of annuli between vulva and anus; **Ran** = number of annuli on tail; **V** = (distance from anterior end to vulva/body length) × 100; **VL/VB** = distance between vulva and posterior end of body divided by body width at vulva; **T** = (distance from cloacal aperture to anterior end of testis/body length) × 100 (Archidona-Yuste et al. 2023, 2024). The raw photographs were edited using Adobe Photoshop v. 24.7.2 (Adobe Inc., San Francisco, CA, USA).

Molecular analyses

DNA was extracted from single nematode specimens following the methodology outlined by Archidona-Yuste et al. (2023, 2024). In all DNA extractions, the four molecular markers of this *Xenocriconemella* isolate were consistently obtained from the same PCR tube, using a single individual, without exception. Seven female specimens were used for molecular analyses. Although ribosomal markers were not successfully amplified for all individuals, the mitochondrial COI marker was obtained from each specimen.

As in previous studies, primers for ribosomal markers-including the D2-D3 expansion domains of 28S rRNA, the Internal Transcribed Spacer region (ITS) rRNA, and the partial 18S rRNA-as well as the mitochondrial COI marker, were the same as those specified in earlier publications (De Ley et al. 1999; Subbotin et al. 2001; Holterman et al. 2006; Hu et al. 2002; Derycke et al. 2005). The PCR cycling conditions followed those described in previous papers (De Ley et al. 1999; Subbotin et al. 2005; Holterman et al. 2006; Powers et al. 2021). PCR products were processed and sequenced at the Stab Vida sequencing facility (Caparica, Portugal) (see Archidona-Yuste et al. 2024 for details). Sequence chromatograms of all markers were analysed using DNASTAR Lasergene SeqMan v. 7.1.0. Species identity of the DNA sequences obtained in this study was tested by Basic Local Alignment Search Tool (BLAST) at the National Center for Biotechnology Information (NCBI) (Altschul et al. 1990). The resulting sequences have been deposited in the GenBank database under accession numbers specified on the phylogenetic trees.

Species delineation analyses

We used two independent approaches of species delineation to resolve the species boundaries within the *X. macrodora* species-complex including morphometric and molecular data.

Principal component analyses (PCA) was conducted to species delimitation from the morphometric data. We included the new population found in Iran and others already described from species detected in the Iberian Peninsula and Costa Rica in the species delimitation analysis within the genus *Xenocriconemella*. For this analysis and to account for intraspecific variation, apart from that detected in this study, we chose 28 Iberian populations including 13 belonging to *X. iberica*, 11 belonging to *X. paraiberica*, and 3 belonging to *X. pradense* as well as belonging to *X. costaricense* and other to *X. tica* from Costa Rica (Archidona-Yuste et al. 2024; Peraza-Padilla et al. 2024, 2025). All the populations were identified using integrative taxonomy. PCA was constructed upon the following morphological characters: L, stylet length, R, Rst, Roes, Rex, RV, Rvan, Ran, and the ratios a, b, c, V, VL/VB (Archidona-Yuste et al. 2024). We tested for collinearity using the values of the variance inflation factor (VIF) (Montgomery et al. 2012). PCA was performed using the PCA function from package 'FactoMineR' (Le et al. 2008). All data analyses were performed with the R version 4.2.2 (R Core Team 2022; https://www.R-project.org).

Species delimitation with molecular data was conducted by the computation of intra- and inter-species disparity, the P ID liberal and Rosenberg's PAB values, employing the species delimitation plugin implemented in Geneious Prime v2022.1.1. (Geneious, Auckland, New Zealand) (Masters et al. 2011). Molecular variation was assessed by calculating the ratio of the mean genetic distance among individuals within and between species (Masters et al. 2011). The P ID (Liberal) value (Ross et al. 2008) represents the probability that a correct species identification is achieved through optimal sequence alignment (BLAST), the closest genetic distance, or placement (falling within or adjacent to a monophyletic species clade). Taxa with P ID (Liberal) ≥ 0.95 were contemplated to be satisfactorily demarcated (Hamilton et al. 2014). Rosenberg's P_{AB} value indicates the probability that the monophyly of a sequence group has occurred to random branching (Rosenberg 2007).

Phylogenetic analyses

Methods and software programs for sequence alignment, editing and phylogenetic analyses followed the procedures previously detailed in earlier studies, including outgroup selection and tree visualization (Hall 1999; Ronquist and Huelsenbeck 2003; Darriba et al. 2012; Tan et al. 2015; Rambaut 2018; Katoh et al. 2019; Etongwe et al. 2020; Nguyen et al. 2022; Archidona-Yuste et al. 2024; Peraza-Padilla et al. 2024). The best-fit models for each marker were as follows: the general time-reversible model with a gamma-shaped distribution (GTR + G) for the D2-D3 expansion domains of 28S rRNA, the transversional model with a gamma-shaped distribution (TVM + G) for ITS rRNA, the Tamura and Nei model with invariable sites (TRN + I) for the partial 18S rRNA gene, and the transitional model with invariable sites and a gamma-shaped distribution (TIM3 + I + G) for the COI gene.

Results

The unidentified population of *Xenocriconemella* was recovered from soil samples collected from a forested area in northern Iran. Morphological and morphometric

analyses indicated a high degree of similarity with known species within the *X. macrodora* species-complex. However, molecular data revealed distinct genetic features that clearly differentiate this population from previously described species. Based on the integrative evidence from both morphometrical and molecular analyses, this population is herein described as a new species within the genus *Xenocriconemella*.

Species delineation using morphometry

Our PCA results revealed a wide variation among specimens primarily captured by the principal component 1 (PC1) which accounted for 80.8% of the total variance in the morphometric characteristics of the *Xenocriconemella macrodora*-complex (Fig. 1A). This PC1 was mainly dominated by body annulation features such as R and Rst, as well as the ratio VL/VB (Fig. 1B). However, we did not detect a clear separation among species within the *X. macrodora*-complex, as all specimens were distributed at random along this component (Fig. 1A). Consequently, we supported the idea that the previously described species (i.e. *X. iberica*, *X. paraiberica*, *X. pradense*, *X. andreae*, *X. tica* and *X. costaricense*) together with the new one described in this study (i.e. *X. persica* sp. nov.) encompass the *X. macrodora*-complex as a model complex of cryptic species Rica (Archidona-Yuste et al. 2024; Cantalapiedra-Navarrete et al. 2024; Peraza-Padilla et al. 2024, 2025). However, it is important to note a certain graphical separation between species along PC2 (dominated by the ratios c and c` as well as the stylet length; Fig. 1B), although this accounted for a low percentage of the variation (9.0%; Fig 1A). This separation was essentially between *X. persica* sp. nov. and the species found in the Iberian Peninsula, such as *X. andreae*, *X. iberica*, *X. paraiberica* and *X. pradense*) (Fig. 1A).

Species delineation using ribosomal and mitochondrial DNA

Species delineation based on ribosomal and mitochondrial markers confirmed that *X. persica* sp. nov., *X. andreae*, *X. iberica*, *X. paraiberica*, *X. pradense*, *X. costaricense*, and *X. tica* are clearly distinguishable from one another, as well as from *X. macrodora* populations in the USA and Italy. The ratio of intra- and inter-species molecular variation for the D2-D3 expansion domains of 28S rRNA and ITS region across all *Xenocriconemella* species was consistently low (0.01–0.09), except for 28S rRNA of *X. costaricense* (0.12) and ITS region of *X. tica* (0.14). By contrast, COI variation was highest in *X. macrodora* (0.34), followed by *X. paraiberica* (0.22), *X. pradense* (0.08), *X. iberica* (0.07), *X. persica* sp. nov. (0.06), and *X. costaricense* (0.03) and *X. tica* (0.03), indicating that COI shows greater genetic diversity in USA populations compared with those from the

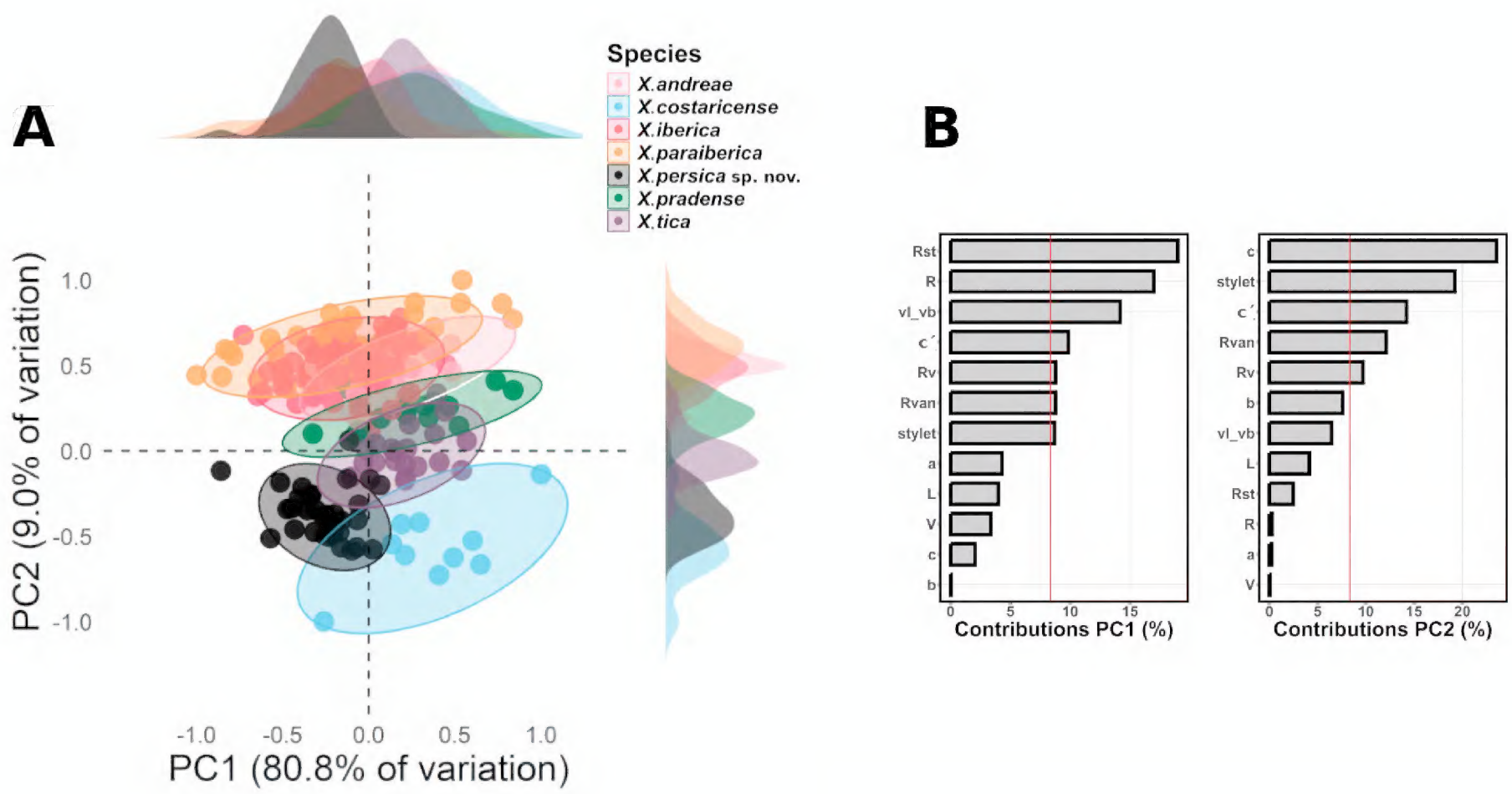

Figure 1. Principal component on *Xenocriconemella macrodora* species-complex. **A.** Projections of species on the plane of components 1 and 2. Density plots on the top and right sides of the ordination plots indicate the scores distribution per species at each principal component. **B.** Barplots showing the standardized contribution (%) of morphometric variables for the PC1 and PC2 (only dimensions with sum of squares (SS) loadings > 1 were extracted). A reference soil (red) line is also shown on the barplot. This reference line corresponds to the expected value if the contribution where uniform. For a given dimension, any row/column with a contribution above the reference line could be considered as important in contributing to the component.

Table 1. Parameters for evaluating species delimitation within *Xenocriconemella* species-complex, based on two rRNA genes (D2-D3 expansion segments of the 28S rRNA and ITS) and one mtDNA barcoding locus, COI, across eight *Xenocriconemella* species.

Species	Gene	Closest species	Intra/ Inter [a]	P ID (Liberal) [b]	Clade Support [c]	Rosenberg's P_{AB} [d]
Xenocriconemella macrodora	D2-D3	–	–	–	–	–
	ITS	–	–	–	–	–
	COI	*X. iberica*	0.34	**0.97 (0.94, 0.99)** [e]	**1.00**	**2.6×10^{-12}**
Xenocriconemella andreae	D2-D3	*X. paraiberica*	0.09	**0.98 (0.93, 1.0)**	**1.00**	**7.3×10^{-14}**
	ITS	*X. paraiberica*	0.02	**0.98 (0.87, 1.0)**	**1.00**	**2.8×10^{-5}**
	COI	*X. iberica*	0.19	**0.96 (0.85, 1.0)**	**1.00**	**3.6×10^{-12}**
Xenocriconemella costaricense	D2-D3	*X. tica*	0.12	**0.95 (0.84, 1.0)**	**1.00**	**2.0×10^{-3}**
	ITS	*X. tica*	0.04	**0.96 (0.81, 1.0)**	**1.00**	0.05
	COI	*X. tica*	0.03	**0.97 (0.86, 1.0)**	**1.00**	**4.1×10^{-3}**
Xenocriconemella iberica	D2-D3	***X. persica* sp. nov.**	0.06	**0.99 (0.97, 1.0)**	**1.00**	**3.7×10^{-20}**
	ITS	***X. persica* sp. nov.**	0.01	**0.98 (0.88, 1.0)**	**1.00**	**2.8×10^{-5}**
	COI	***X. persica* sp. nov.**	0.07	**0.99 (0.96, 1.0)**	NA	NA
Xenocriconemella paraiberica	D2-D3	*X. persica*	0.05	**1.00 (0.97, 1.0)**	**1.00**	**2.2×10^{-12}**
	ITS	*X. tica*	0.03	**1.00 (0.96, 1.0)**	**1.00**	**4.7×10^{-10}**
	COI	*X. iberica*	0.22	**0.97 (0.95, 1.0)**	**1.00**	**1.6×10^{-31}**
***Xenocriconemella persica* sp. nov.**	D2-D3	*X. pradense*	0.08	**0.97 (0.87, 1.0)**	**1.00**	0.05
	ITS	*X. pradense*	0.02	**1.00 (0.85, 1.0)**	**1.00**	**3.0×10^{-3}**
	COI	*X. iberica*	0.04	**0.99 (0.93, 1.0)**	**1.00**	NA
Xenocriconemella pradense	D2-D3	***X. persica* sp. nov.**	0.03	**1.00 (0.97, 1.0)**	**1.00**	**3.7×10^{-7}**
	ITS	***X. persica* sp. nov.**	0.02	**0.98 (0.87, 1.0)**	**1.00**	**3.0×10^{-3}**
	COI	*X. iberica*	0.08	**0.98 (0.93, 1.0)**	**1.00**	**9.9×10^{-17}**
Xenocriconemella tica	D2-D3	*X. costaricense*	0.09	**0.97 (0.87, 1.0)**	**1.00**	**2.0×10^{-3}**
	ITS	*X. costaricense*	0.14	**0.93 (0.79, 1.0)**	**1.00**	0.05
	COI	*X. costaricense*	0.03	**0.97 (0.86, 1.0)**	**1.00**	**4.1×10^{-3}**

[a] Intraspecific variation relative to interspecific variation. [b] The P ID (Liberal) value represents the probability (with the 95% confidence interval) for the prediction of making a correct identification of an unknown specimen of the focal species using DNA Barcoding (closest genetic distance). P ID (Liberal) values ≥ 0.95 were considered to be significant delimited (Hamilton et al. 2014). Numbers in bold represent significant values. [c] Clade support: posterior probabilities from Bayesian trees. [d] Rosenberg's P_{AB} value is the probability that the monophyly of a group of sequences is the result of random branching, Rosenberg's significant values = $P \leq 0.05$. [e] Significant results are indicated in bold. (-) Not obtained or not performed because only a single sequence of D2-D3 or ITS for this species is available in NCBI. NA: not available due to cladistics related to calculations in the test.

Iberian Peninsula and Costa Rica populations (Table 1). For all eight species, the D2-D3 expansion domains of 28S rRNA and ITS genes exhibited consistently low intra- and inter-species molecular variation (Table 1), indicating that these loci are highly effective for species separation (Ross et al. 2008). Similarly, P ID (Liberal) values for all eight species and loci were ≥ 0.95, except for COI in *X. iberica* and *X. persica* sp. nov., demonstrating that these *Xenocriconemella* species are adequately delineated (Ross et al. 2008; Hamilton et al. 2014). The P ID (Liberal) value (Ross et al. 2008) represents the probability of accurate species identification using BLAST, the closest genetic distance, or phylogenetic placement within a monophyletic species clade. Species with P ID (Liberal) ≥ 0.95 were deemed to be adequately delimited (Hamilton et al. 2014). Additionally, all clades were well-supported [Bayesian posterior probability (BPP) = 1.00] in the phylogenetic trees across all three loci, while Rosenberg's PAB values also confirmed monophyly ($P < 0.05$) for all eight species (Rosenberg 2007), except for COI in *X. iberica* and *X. persica* sp. nov. (Table 1).

Ribosomal and mitochondrial DNA characterization

Xenocriconemella persica sp. nov. was molecularly characterized using sequences from three ribosomal genes, the D2-D3 expansion domains of 28S rRNA, ITS rRNA, and partial 18S rRNA, as well as the mitochondrial gene COI. For this new species, six D2-D3 expansion domains sequences of 28S rRNA (663–708 bp; PV744360–PV744365), three ITS rRNA sequences (778 bp; PV744366–PV744368), three 18S rRNA sequences (1630–1703 bp; PV744369–PV744371), and seven COI sequences (330–361 bp; PV743275–PV743281) were obtained. Intraspecific sequence variation was low across both ribosomal and mitochondrial markers: D2-D3 expansion domains of 28S rRNA (99.9–100.0%, 0–1 bp and 0–1 indels); ITS rRNA, partial 18S rRNA; and COI with no intraspecific variability detected (100.0 similarity). D2-D3 expansion domains of 28S rRNA of *X. persica* sp. nov. (PV744360–PV744365) exhibited: 96.5% similarity to *X. macrodora* from Italy

(AY780960), differing by 19 bp and 2 indels, and 77% coverage; 94.9% similarity to *X. pradense* from Spain (OR880202–OR880217), differing by 36 bp and 2 indels; 94.1–94.5% similarity to *X. iberica* from Spain (OR880107–OR880148), differing by 39–40 bp and 4 indels; 92.7–92.9% similarity to *X. andreae* from Spain and Portugal (PP833567–PP833576), differing by 50–51 bp and 3 indels; 92.0–92.3% similarity to *X. paraiberica* from Spain (OR880152–OR880199), differing by 54–56 bp and 3–5 indels; 91.4% similarity to *X. tica* from Costa Rica (PV435862–PV435866), differing by 61 bp and 3 indels; and 90.7–91.0% similarity to *X. costaricense* from Costa Rica (PP209388–PP209391), differing by 64–65 bp and 3 indels (Subbotin et al., 2005; Archidona-Yuste et al. 2024; Cantalapiedra-Navarrete et al. 2024; Peraza-Padilla et al. 2024; 2025). The ITS sequences of *X. persica* sp. nov. (PV744366–PV744368) were most similar to: *X. pradense* (90.4%; differing by 76 bp and 18 indels; OR878350); *X. iberica* (86.9–87.5%; differing by 91–105 bp and 26–33 indels; OR878332–OR878336); *X. costaricense* (83.0%; differing by 130 bp and 32 indels; PP209397, PP209398); *X. andreae* (80.8–85.7%; differing by 87–159 bp and 27–61 indels; PP833563–PP833565); *X. tica* (80.9–81.1%; differing by 142–145 bp and 52 indels; PV435912–PV435914); *X. paraiberica* (79.0–79.2%; differing by 177–179 bp and 91–92 indels; OR878346–OR878349); *X. macrodora* (77.9%; differing by 92 bp and 37 indels; JQ708139) with low coverage (52%). Partial 18S rRNA of *X. persica* sp. nov. (PV744369–PV744371) showed 99.4–99.5% similarity to *X. pradense* (OR878360–OR878361), differing by 9–10 bp and 2 indels); 99.0% similarity to *X. iberica* (OR878356), differing by 17 bp and 2 indels; 98.3% similarity to *X. paraiberica* (OR878358), differing by 29 bp and 6 indels; 98.2% similarity to *X. macrodora* (MF094906, MF094973, MF095001), differing by 30–31 bp and 6 indels; 97.1–97.8% similarity to *X. costaricense* (PP209392–PP209396), differing by 38–43 bp and 6–7 indels; 97.5–97.8% similarity to *X. andreae* (PP833577–PP833580), differing by 38–42 bp and 7 indels; and 92.0% similarity to *X. tica* (PV435890–PV435893), differing by 34 bp and 6 indels. Finally, COI sequences of *X. persica* sp. nov. (PV743275–PV743281) displayed: 91.5–92.5% similarity to *X. iberica* from Spain and Portugal (OR885936–OR885976), differing by 22–26 bp and 2 indels; 88.1–90.6% similarity to *X. paraiberica* from Spain (OR885983–OR886017), differing by 31–39 bp and 0 indel; 88.6–89.42% similarity to *X. pradense* from Spain (OR886020–OR886029), differing by 37–40 bp and 0 indel; 85.5–88.9% similarity to *X. macrodora* from USA (MF770894–MF770950, MN711386–MN711444) (differing by 40–52 bp and 0 indel; 87.2–88.2% similarity to *X. andreae* from Portugal and Spain (PP831172–PP831177), differing by 35–38 bp and 0 indel; 87.0% similarity to *X. costaricense* from Costa Rica (PP210897–PP210900), differing by 41 bp and 0 indel; and 86.3% similarity to *X. tica* from Costa Rica (PV210897–PV210900), differing by 45 bp and 0 indel.

Phylogenetic analysis

Phylogenetic analysis of *Xenocriconemella* species, based on the D2-D3 expansion domains of 28S, ITS rRNA, partial 18S rRNA, and the partial COI mtDNA sequences, was conducted using BI (Figs 2, 3, 4 and 5, respectively). The phylogenetic trees constructed from the ribosomal and mitochondrial DNA markers included 141, 39, 36 and 186 sequences, with alignments consisting of 704, 800, 1705, and 362 characters, respectively. The Bayesian 50% majority-rule consensus tree inferred from the D2-D3 expansion domains of 28S rRNA is shown in Fig. 2. For this ribosomal marker, all eight species within the genus *Xenocriconemella* clustered within a well-supported clade (BPP = 1.00) (Fig. 2). The *Xenocriconemella* clade was further subdivided into two well-supported (BPP = 1.00) subclades (I and II): subclade I includes two species from the Iberian Peninsula-*X. paraiberica* (OR880152–OR880202) and *X. andreae* (PP833567–PP833576)-as well as two species from Costa Rica-*X. costaricense* (PP209388–PP209391) and *X. tica* (PV435862–PV435866); and subclade II comprises all the sequences for *X. persica* sp. nov. (PV744360–PV744365), *X. pradense* (OR880203–OR880218), *X. iberica* (OR880107–OR880150), and the single sequence of *X. macrodora* from Italy (AY780960).

In the ITS region tree (Fig. 3), phylogenetic analysis revealed that all *Xenocriconemella* species formed a well-supported clade (BPP = 1.00), except for *X. macrodora* from the USA (JQ708139), which was clearly separated from the other *Xenocriconemella* species. This big clade was subdivided into several subclades, including one well-supported subclade (BPP = 1.00) that grouped *X. persica* sp. nov. (PV744366–PV744368) together with two Iberian Peninsula species, *X. iberica* (OR878332–OR878337) and *X. pradense* (OR878350–OR878355). However, the other two Iberian Peninsula species, *X. andreae* (PP833563–PP833566) and *X. paraiberica* (OR878338–OR878349), clustered separately into distinct subclades. Additionally, the two Costa Rican species, *X. costaricense* (PP209397–PP209398) and *X. tica* (PV435912–PV435914), formed a well-supported subclade (BPP = 1.00) (Fig. 3).

In the 18S rRNA phylogenetic analysis (Fig. 4), all sequences within the genus *Xenocriconemella* clustered into a well-supported clade (BPP = 1.00); however, some subclades lacked strong support (Fig. 4). *Xenocriconemella persica* sp. nov. (PV744369–PV744371) formed a distinct cluster alongside two Iberian Peninsula species, *X. iberica* (OR878356–OR878357) and *X. pradense* (OR878360-OR878361). *Xenocriconemella macrodora* (MF094973, MF095001, MF094906, MF094907, FJ489556, FJ489557, FJ489598, FJ489599, JF972482, HM116004) clustered in a separate subclade with moderate support (BPP = 0.96). Similarly, the two Costa Rican species, *X. costaricense* (PP209392–PP209396) and *X. tica* (PV435890–PV435893), clustered together in a separate subclade with moderate support (BPP = 0.96). Meanwhile, *X. paraiberica* (OR878358–OR878359) and *X. andreae* (PP833577–PP833582) clustered separately into two well-supported subclades (BPP = 1.00) (Fig. 4).

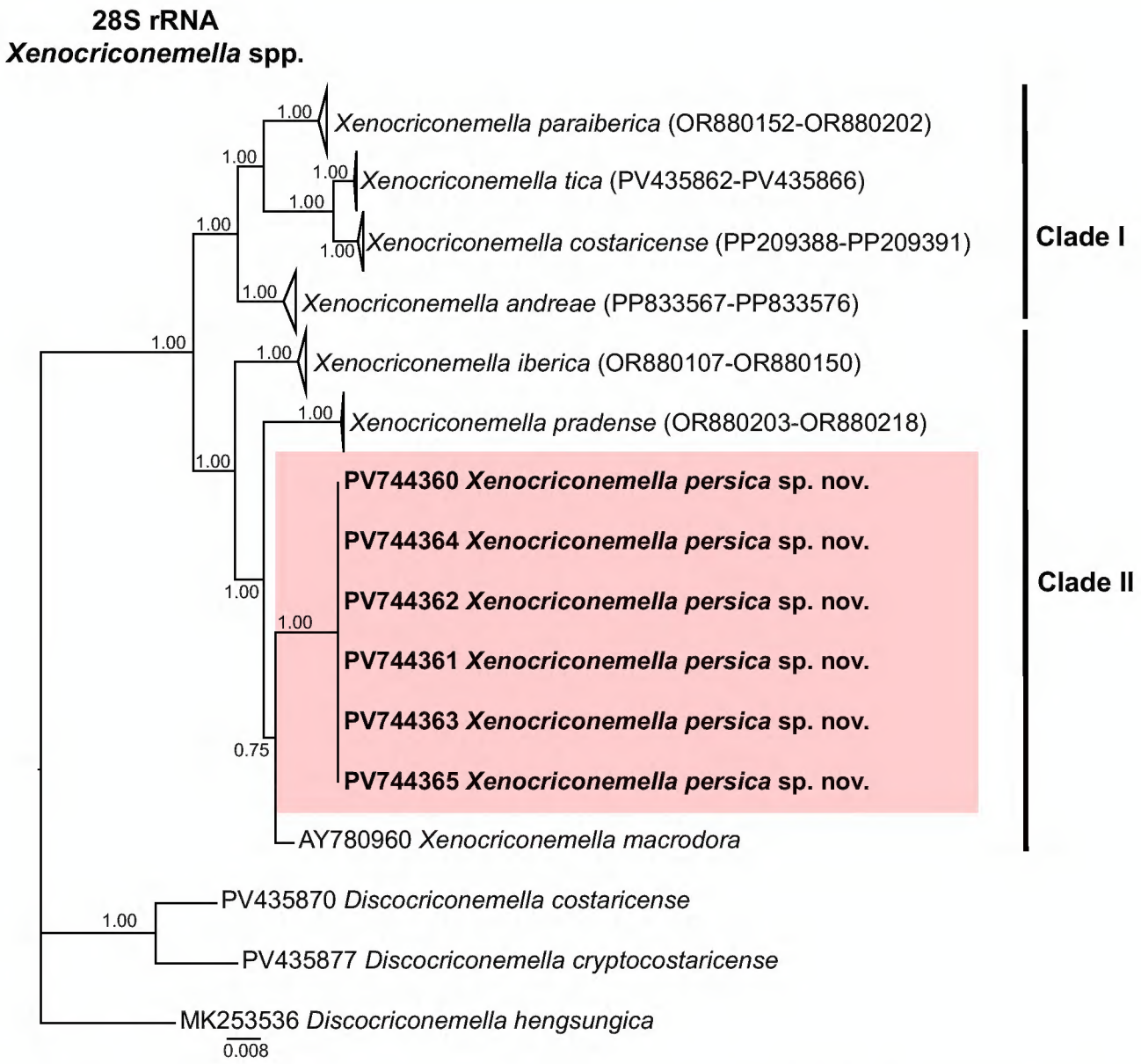

Figure 2. Phylogenetic relationships of *Xenocriconemella persica* sp. nov. with other *Xenocriconemella* spp. Bayesian 50% majority rule consensus tree as inferred from D2 and D3 expansion domains of 28S rRNA sequence alignment under the GTR + G model (−lnL = 2604.7495; AIC = 5787.499000; freqA = 0.1978; freqC = 0.2331; freqG = 0.3307; freqT = 0.2384; R(a) = 0.3647; R(b) = 1.5158; R(c) = 0.5029; R(d) = 0.3687; R(e) = 3.4897; R(f) = 1.0000; Pinva = 0.0000; and Shape = 0.2810). Posterior probabilities more than 0.70 are given for appropriate clades. Newly obtained sequences in this study are shown in bold, and coloured box indicate clade association of the new species. Scale bar = expected changes per site.

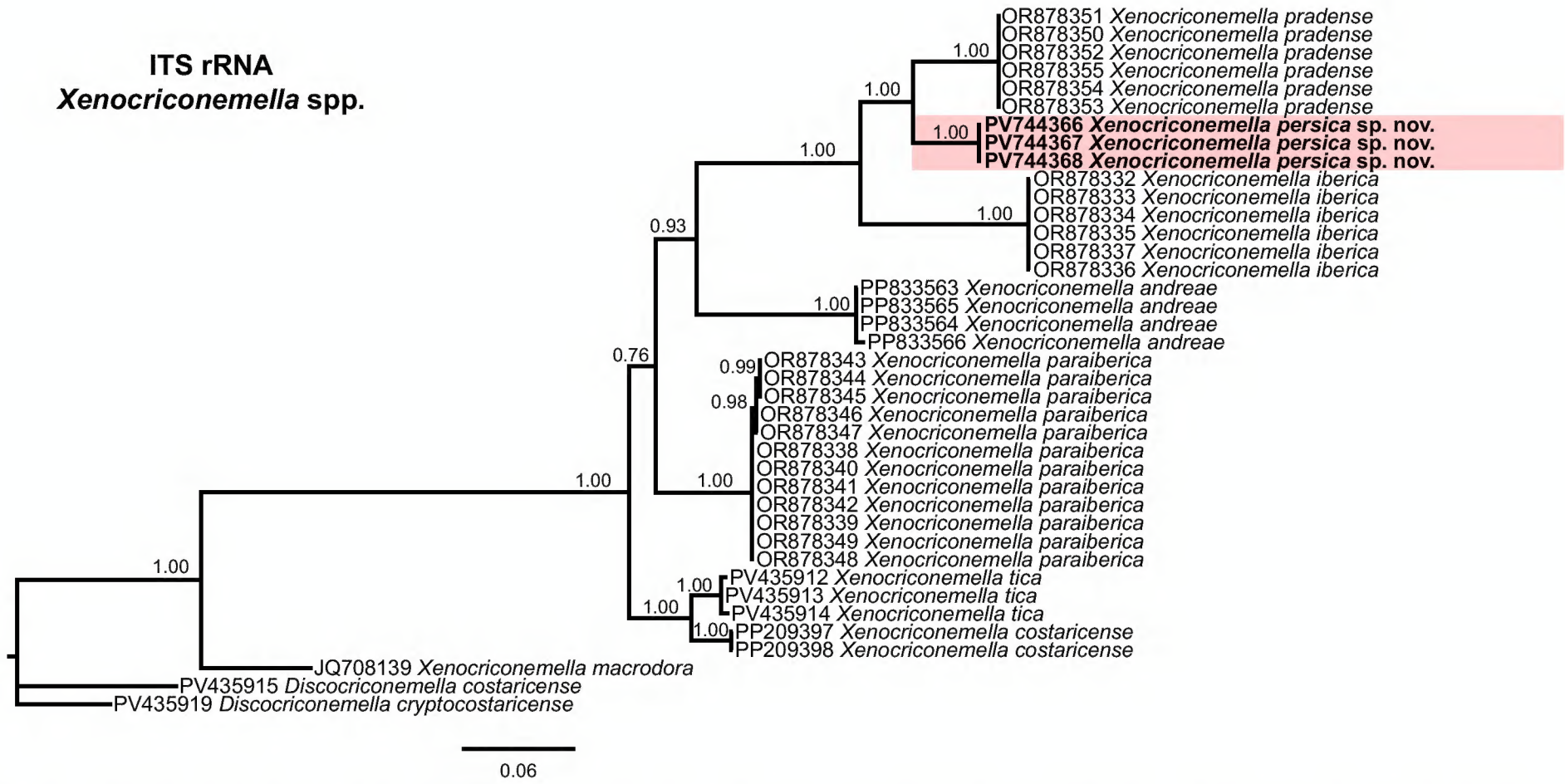

Figure 3. Phylogenetic relationships of *Xenocriconemella persica* sp. nov. with other *Xenocriconemella* spp. Bayesian 50% majority rule consensus tree as inferred from ITS rRNA sequence alignment under the TVM + G model (−lnL = 3811.0906; AIC = 7790.181140; freqA = 0.2026; freqC = 0.2539; freqG = 0.2752; freqT = 0.2684; R(a) = 0.9730; R(b) = 2.3019; R(c) = 1.2919; R(d) = 0.3195; R(e) = 2.3019; R(f) = 1.0000; Pinva = 0.0000; and Shape = 0.3920). Posterior probabilities more than 0.70 are given for appropriate clades. Newly obtained sequences in this study are shown in bold, and coloured box indicate clade association of the new species. Scale bar = expected changes per site.

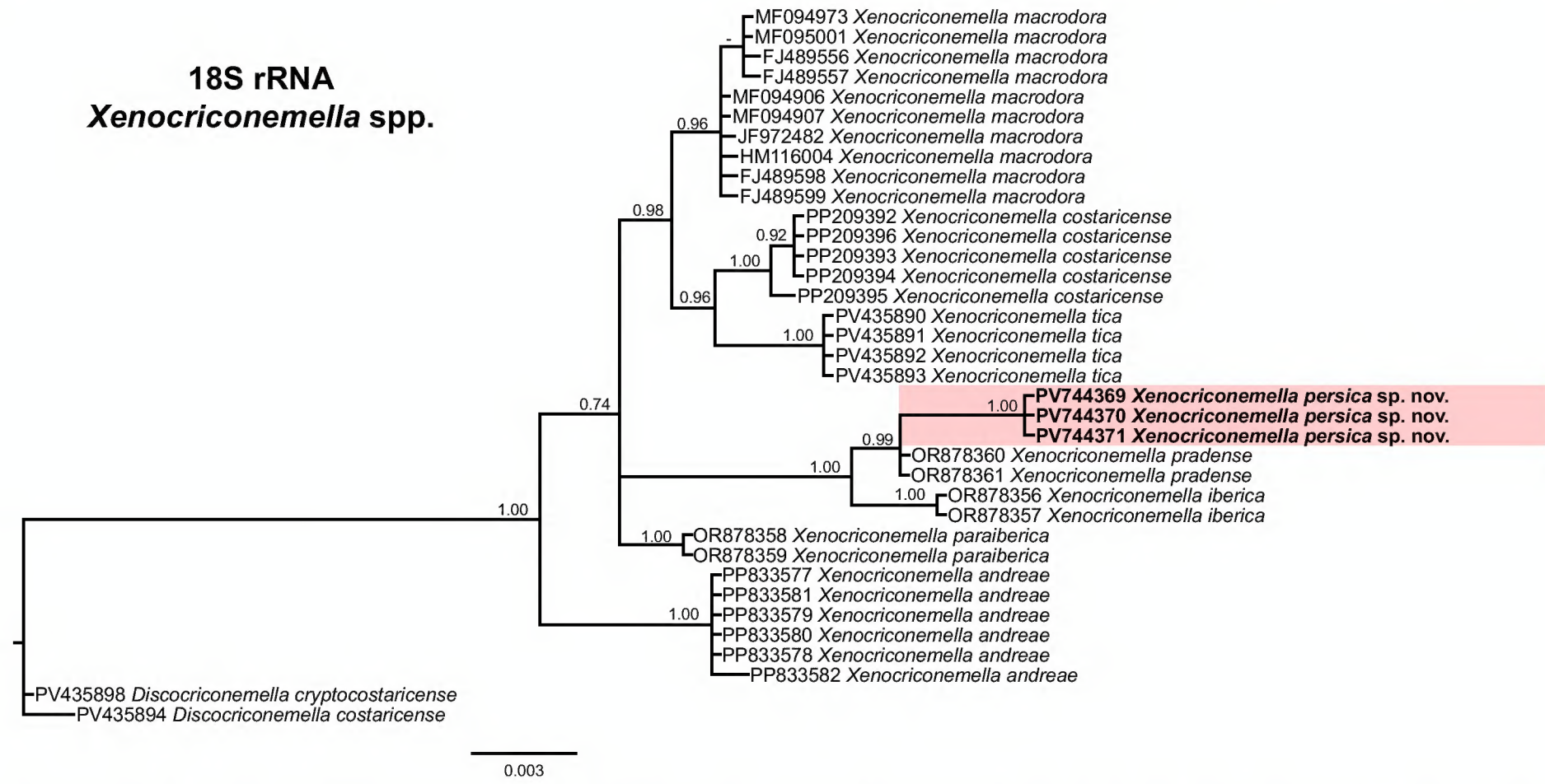

Figure 4. Phylogenetic relationships of *Xenocriconemella persica* sp. nov. with other *Xenocriconemella* spp. Bayesian 50% majority rule consensus tree as inferred from 18S rRNA sequence alignment under the TrN + I model (−lnL = 3086.5512; AIC = 6325.102340; freqA = 0.2368; freqC = 0.2400; freqG = 0.2887; freqT = 0.2346; R(a) = 1.0000; R(b) = 2.5960; R(c) = 1.0000; R(d) = 1.0000; R(e) = 6.7320; R(f) = 1.0000; Pinva = 0.9000). Posterior probabilities more than 0.70 are given for appropriate clades. Newly obtained sequences in this study are shown in bold, and coloured box indicate clade association of the new species. Scale bar = expected changes per site.

Although phylogenetic relationships on the COI gene were not well resolved, all *Xenocriconemella* sequences clustered within a well-supported clade (BPP = 1.00) (Fig. 5). The phylogenetic position of *X. persica* sp. nov. was distinct, forming a separated subclade from other species within the genus (BPP = 1.00). Sequences of *X. macrodora* from the USA, *X. costaricense* and *X. tica*, *X. paraiberica*, *X. pradense*, and *X. andreae*, clustered together in an unresolved subclade (BPP = 0.78), while *X. iberica* occupied a basal position in this clade (Fig. 5).

Taxonomy

Phylum: Nematoda Rudolphi, 1808
Class: Chromadorea Inglis, 1983
Order: Rhabditida Chitwood, 1933
Suborder: Tylenchina Chitwood, 1950
Superfamily: Criconematoidea Khan & Ahmad, 1975
Family: Criconematidae Taylor, 1936
Genus: *Xenocriconemella* De Grisse & Loof, 1965

***Xenocriconemella persica* sp. nov.**

https://zoobank.org/7D3FE7B0-DCB5-4A05-BCA4-9329F0F3D17B

Description. Females. Body ventrally arcuate to straight, slightly narrowing anteriorly and posteriorly. Body annuli smooth and retrorse 2.5 (2.0–3.0) µm wide, rarely with anastomosis (in four nematode specimens, a single anastomosis was observed in the tail and stylet knob regions). Lip region with two annuli, not offset, not separated from body contour, first lip annulus partially covering the second lip annulus (Figs 6, 7), second lip annulus retrorse and slightly wider than first annulus 8.1 (7.0–9.0) µm wide. Stylet thin, long, and flexible (Figs 6, 7; Table 2), occupying 33.8 (28.4–37.0) % of the body length, with short basal portion 6.2 (5.0–7.0) µm long, and knobs slightly rounded 4.3 (3.0–5.5) µm wide. Pharynx typical criconematoid, with a cylindroid procorpus widening to a large muscular oval median bulb containing well developed valves (8.0–9.0 µm long), isthmus slender and amalgamated with basal bulb. Excretory pore located from one to nine annuli anterior to level of stylet knobs, with an average of 4 annuli, at 89.6 (88.0–100.0) µm from anterior end. Nerve ring located at the level of isthmus, 105.7 (97.0–111.0) µm from the anterior end. Vagina ventrally curved (10.0–14.0 µm long). Female genital tract monodelphic, prodelphic, outstretched and occupying 43.0 (30.2–46.1) % of the body length, spermatheca almost hemispherical (9.0–14.0 × 9.0–14.0) µm, sperm absent. Anus located at 7.6 (6–9) annuli from the terminus. Tail short, conoid, with bluntly rounded terminus.

Males. Not found.

Juveniles. Body like females, including tail shape, but shorter. Edge of body annuli without appendages, but noticeable delicate irregular punctations.

Diagnosis and relationships. *Xenocriconemella persica* sp. nov. is characterized by the following measurements and ratios: a short-sized female body 287 (234–316) µm, a long and flexible stylet = 96.8 (83.0–103.0) µm long, V = 88.5 (86.7–91.0), a = 9.8 (7.6–11.5),

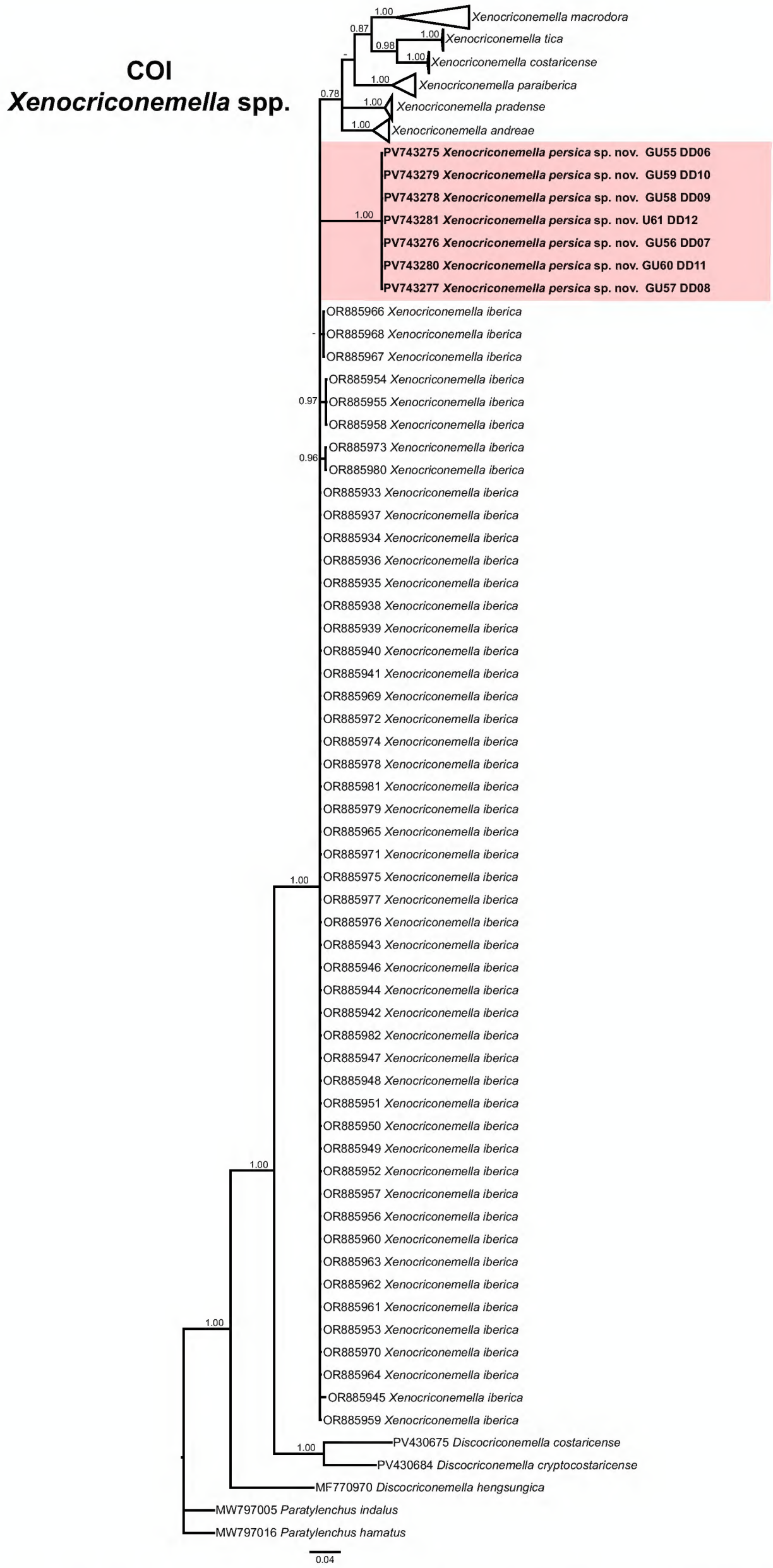

Figure 5. Phylogenetic relationships of *Xenocriconemella persica* sp. nov. with other *Xenocriconemella* spp. Bayesian 50% majority-rule consensus trees as inferred from cytochrome c oxidase subunit I (COI) mtDNA gene sequence alignments under the TIM3 + I + G model (−lnL = 2708.4540; AIC = 6172.907980; freqA = 0.3893; freqC = 0.0358; freqG = 0.0779; freqT = 0.4971; R(a) = 4.0721; R(b) = 12.1432; R(c) = 1.0000; R(d) = 4.0721; R(e) = 24.7120; R(f) = 1.0000; Pinva = 0.3920; and Shape = 0.4580). Posterior probabilities more than 0.70 are given for appropriate clades. Newly obtained sequences in this study are shown in bold, and coloured box indicate clade association of the new species. Scale bar = expected changes per site.

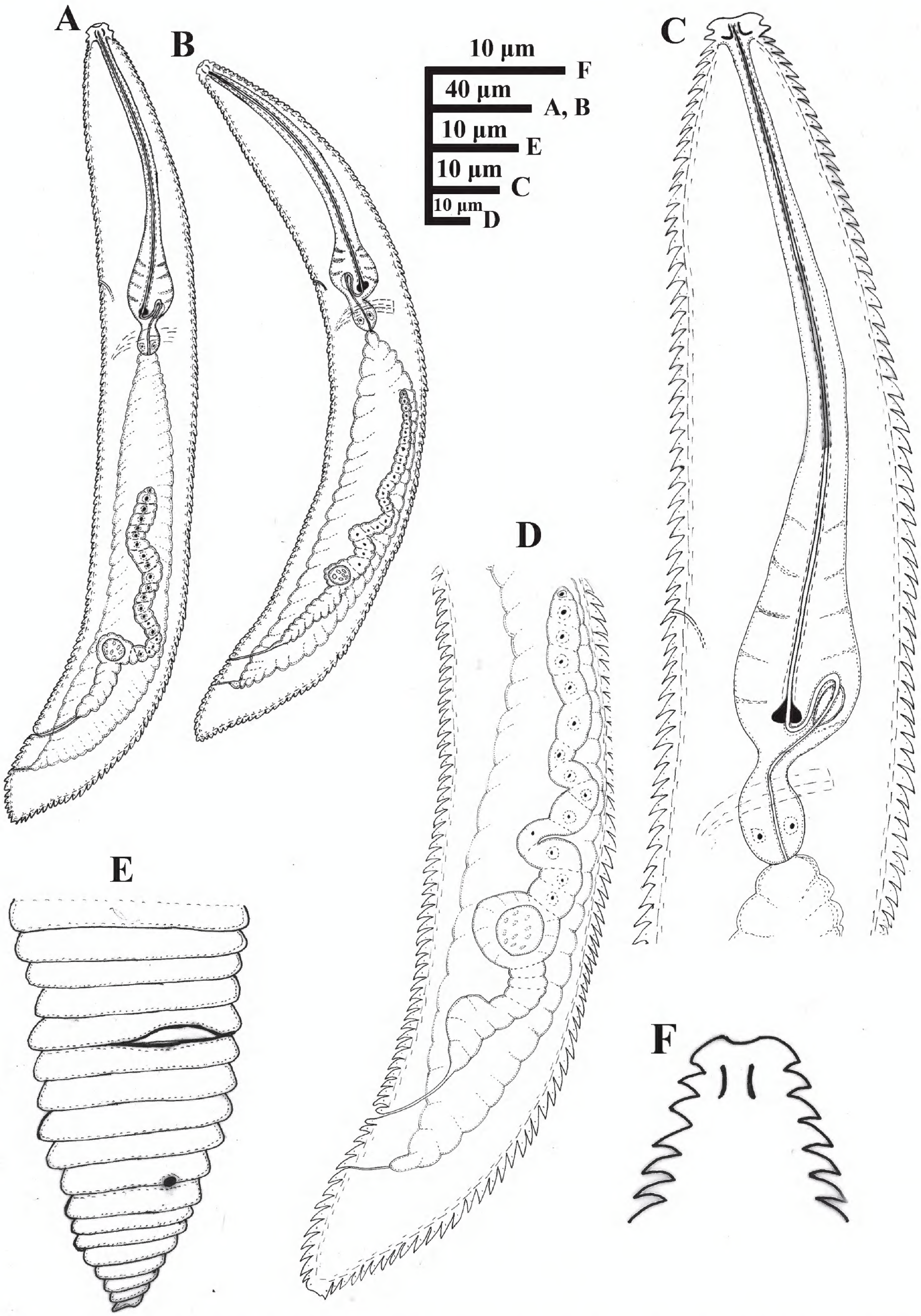

Figure 6. *Xenocriconemella persica* sp. nov. (drawings). **A, B.** Entire female; **C.** Female anterior region; **D.** Female posterior region showing gonad; **E.** Detail of female posterior region showing vulva and anus; **F.** Detail of lip region.

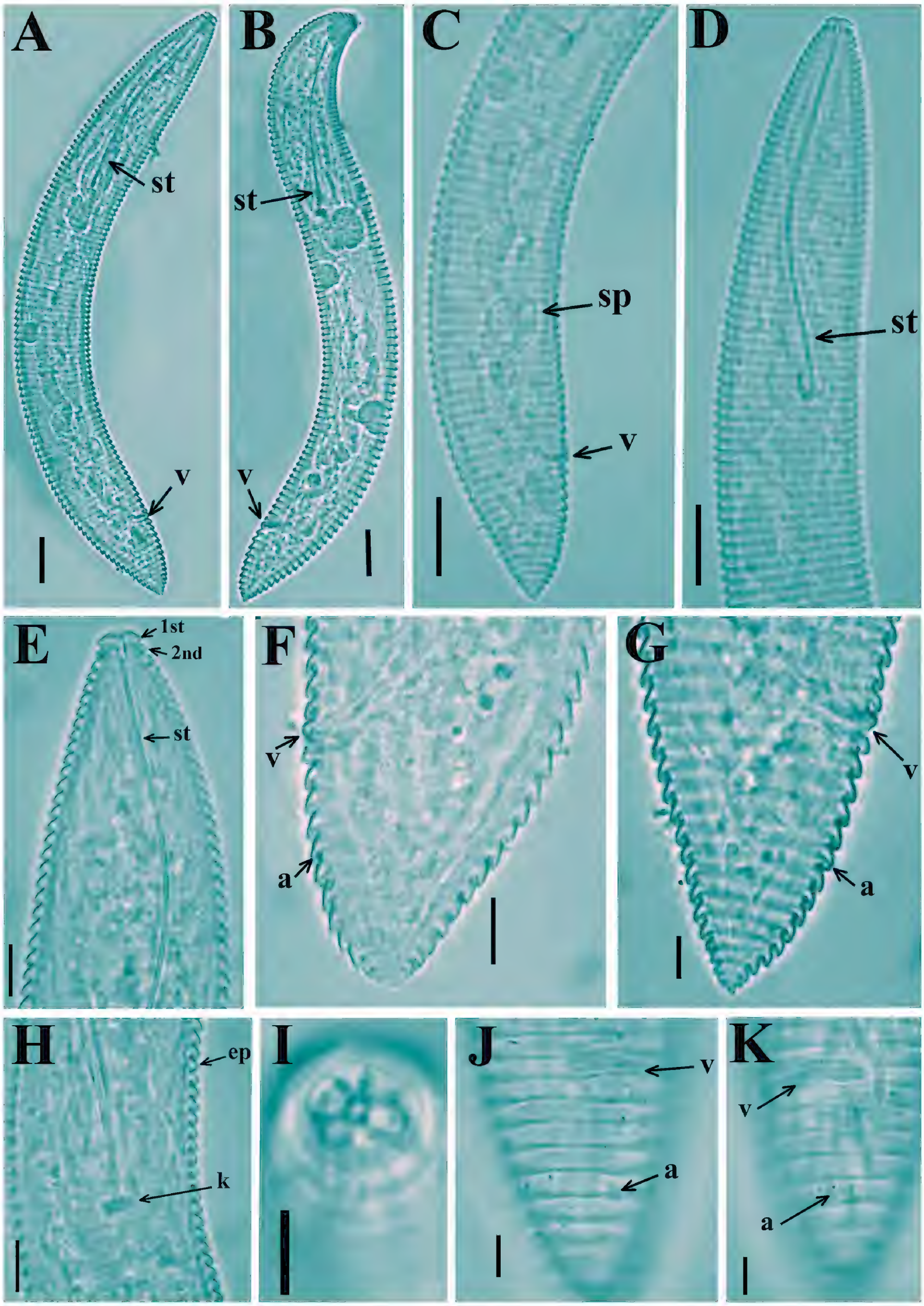

Figure 7. Light micrographs of *Xenocriconemella persica* sp. nov. **A, B.** Entire female showing stylet and vulva (arrowed); **C.** Female posterior body region showing vulva and spermatheca (arrowed); **D.** Female anterior body region showing stylet (arrowed); **E.** Detail of female lip region showing 1st and 2nd annuli (arrowed); **F, G, J, K.** Vulval region showing vulva and anus (arrowed); **H.** Detail of pharyngeal region showing secretory-excretory pore and stylet knobs (arrowed); **I.** *En face* view. Abbreviations: a = anus; ep = secretory-excretory pore; k = stylet knobs; sp = spermatheca; st = stylet; V = vulva; 1st and 2nd, first and second body annuli. Scale bars: 20 µm (**A–D**); 10 µm (**E, F, H**); 5 µm (**G, I–K**).

Table 2. Morphometrics of *Xenocriconemella persica* sp. nov. from the rhizosphere of forest trees (*Alnus glutinosa* (L.) Gaertn., and *Fagus orientalis* Lipsky) at Pounel, Rezvanshahr County, Gilan province, Iran[1].

Character[1]	Holotype	Paratype Females
N	1	32
L	280	286.6 ± 17.1 (234–316)
R	114	111.9 ± 5.0 (104–124)
Rst	40	42.6 ± 1.8 (41–49)
Roes	49	57.2 ± 2.2 (39–49)
Rex	38	38.3 ± 1.9 (35–43)
RV	13	13.2 ± 1.0 (11–15)
Rvan	4	4.7 ± 0.6 (4–6)
Ran	9	7.6 ± 0.9 (6–9)
O	8.7	7.3 ± 0.9 (5.9–9.3)
A	11.2	9.8 ± 1.2 (7.6–11.5)
B	2.5	2.4 ± 0.1 (2.0–2.7)
C	16.5	18.9 ± 2.7 (14.6–25.5)
c'	0.8	0.9 ± 0.1 (0.6–1.1)
V	88.9	88.5 ± 1.0 (86.7–91.0)
VL/VB	0.9	1.3 ± 0.2 (0.9–1.7)
Stylet	92.0	96.8 ± 4.9 (83.0–103.0)
Pharynx	112.0	117.9 ± 4.0 (110–125)
Max. body width	25.0	29.7 ± 3.9 (24.0–38.0)
Anal body width	19.0	18.2 ± 1.3 (16.0–20.0)
Vulva to anus distance	16.0	17.5 ± 3.5 (7.0–24.0)
Tail	17.0	15.4 ± 2.1 (11.0–20.0)

[1]All measurements are in µm and in the form: mean ± s.d. (range).

b = 2.4 (2.0–2.7), c = 18.9 (14.6–25.5), c' = 0.9 (0.6–1.1), R = 111.9 (104–124), RV = 13.2 (11–15), Ran = 7.6 (6–9), VL/VB = 1.3 (0.9–1.7). Morphologically and morphometrically, *X. persica* sp. nov. resembles *X. pradense* and all other members of the *X. macrodora* species-complex (including *X. macrodora*, *X. andreae*, *X. iberica X. paraiberica*, *X. costaricense*, and *X. tica*) from which it is very difficult to separate, but can be separated by several morphometric traits and ratio, and molecular markers. From *X. pradense* mainly differs by a slightly shorter body length 287 (234–316) µm vs. 333 (249–383) µm, a slightly lower number of body annuli 112 (104–124) vs. 122 (112–128), a slightly shorter stylet length 96.8 (83.0–103.0) µm vs 100.5 (92.5–110.0) µm, an anterior position of the excretory pore 0–9 annuli anterior to level of stylet knobs vs. one annulus posterior to level of stylet knobs, a lower number of body annuli from vulva to posterior end (RV) 13.2 (11–15) vs. 15.9 (15–18), a slightly shorter tail length 15.4 (11.0–20.0) µm vs. 19.9 (15.5–25.0) µm, and a slightly higher c ratio 18.9 (14.6–25.5) vs. 16.6 (13.7–21.3). From *X. macrodora* it is almost undistinguishable (Table 2, Archidona-Yuste et al. 2024). And it is also quite close to *X. andreae*, but differs by a slightly shorter body length 287 (234–316) µm vs. 307 (274–353) µm, a higher number of annuli between vulva and anus (RVan) 4.7 (4–6) vs 3 (3–3), and a slightly longer tail length 15.4 (11.0–20.0) µm vs 11.9 (10.0–14.0) µm. From *X. iberica* it differs also slightly in some main diagnostic characters, including a slightly larger stylet length 96.8 (83.0–103.0) µm vs 93.1 (80.0–103.0) µm, a slightly higher number of body annuli (R) 111.9 (104–124) vs 104 (97–119), and a slightly higher VL/VB ratio 1.3 (0.9–1.1) vs 1.2 (0.7–1.4). From *X. paraiberica* it is also almost undistinguishable, but mainly differs by a slightly longer stylet length 96.8 (83.0–103.0) µm vs 89.6 (80.0–100.0) µm, a higher number of body annuli (R) 111.9 (104–124) vs 104 (95–116), and a slightly lower c ratio 18.9 (14.6–25.5) vs 20.2 (13.0–28.6). Finally, from *X. costaricense* and *X. tica* clearly differs by a shorter body length 287 (234–316) µm vs 349 (276–404), 324 (271–358) µm, respectively, a shorter stylet length 96.8 (83.0–103.0) µm vs 125 (113.0–133.0), 117 (112.0–123.5) µm, respectively, a slightly lower and higher, respectively, number of body annuli (R) 111.9 (104–124) vs 124 (117–130), 103 (98–108), a slightly lower c ratio 18.9 (14.6–25.5) vs 22.8 (16.0–28.8), 25.3 (19.5–31.6), respectively, and a slightly higher VL/VB ratio 1.3 (0.9–1.7) vs 1.1 (0.9–1.3), 1.2 (0.8–1.5), respectively. In any case, these minor differences are within the range of the *X. macrodora* species-complex, and all eight species need to be considered as a complex of cryptic species which are well resolved by morphometric and molecular analyses (see above morphometric and molecular studies).

Etymology. The species epithet refers to Persia, the Latin name of Iran, the country of origin.

Type host and locality. The new species was recovered from the rhizosphere of forest trees (*Alnus glutinosa* (L.) Gaertn., and *Fagus orientalis* Lipsky) at Pounel- Khalkhal road, Rezvanshahr County, Gilan province, Iran (coordinates 37°32'17.6"N, 48°51'28.9"E, 750 m a.s.l.).

Type material. • Holotype female (slide 0207B-5) and 20 female paratypes (slides 0207B-1-0207B-5) deposited at the Nematode Collection of the Faculty of Agriculture, University of Zanjan, Zanjan, Iran • 10 female paratypes (slides Xe_Ir-01- Xe_Ir-05) at nematode collection of Institute for Sustainable Agriculture (IAS) of Spanish National Research Council (CSIC), Córdoba, Spain; and two females at the USDA Nematode Collection (slide T-8278p).

Discussion

Xenocriconemella species feed ectoparasitically on root tips or along mature roots. These nematodes are migratory, and their feeding activity can impair root function, diminishing the plant's capacity to absorb water and nutrients. Such damage may result in stunted growth or chlorosis. However, their economic impact remains poorly studied and is generally considered limited, likely due to their typically low population densities in natural soils (Archidona-Yuste et al. 2024). This study reports the discovery and integrative characterisation of a new cryptic species of *Xenocriconemella* from natural forests in northern Iran. Morphological and morphometric analyses revealed close affinities with species belonging to the *X. macrodora* species-complex.

However, molecular markers, based on ribosomal and mitochondrial, clearly distinguished the new Iranian population from all other species within this genus, confirming its status as a new valid species within the genus *Xenocriconemella*. Additionally, the species delimitation methods employed in this study support the recognition of this taxon as a new and valid species. However, some of the tests presented limitations related to the COI marker, particularly regarding the clade position inferred for this population of *X. persica* sp. nov. These findings underscore the importance of integrating morphological and molecular approaches for accurate species delimitation in cryptic taxa, particularly in genera like *Xenocriconemella*, where morphological differences are subtle. Moreover, this study, alongside recent integrative taxonomic investigations of *X. macrodora*-complex populations from multiple countries, provides compelling evidence that the previously recognised cosmopolitan species *X. macrodora* should be redefined as a species complex. This complex includes at least eight species: *X. andreae*, *X. costaricense*, *X. iberica*, *X. macrodora*, *X. paraiberica*, *X. persica* sp. nov., *X. pradense*, and *X. tica* (Archidona-Yuste et al. 2024; Peraza-Padilla et al. 2024; Cantalapiedra-Navarrete et al. 2024; Peraza-Padilla et al. 2025).

Ribosomal and mitochondrial markers, including the D2-D3 expansion domains of 28S, ITS rRNA, partial 18S rRNA, and the mtDNA gene COI, remain indispensable tools for accurate species identification within *Xenocriconemella* (Archidona-Yuste et al. 2024; Peraza-Padilla et al. 2024; Cantalapiedra-Navarrete et al. 2024; Peraza-Padilla et al. 2025). Previous phylogenetic analyses based on these markers using BI confirmed the monophyly of the genus *Xenocriconemella* (Subbotin et al. 2005; Etongwe et al. 2020; Nguyen et al. 2022; Archidona-Yuste et al. 2024; Peraza-Padilla et al. 2024; Cantalapiedra-Navarrete et al. 2024; Peraza-Padilla et al. 2025). Phylogenetic analyses consistently placed the newly described species within the *Xenocriconemella* clade, in close association with other members of the *X. macrodora* species-complex. These results further support the hypothesis that *Xenocriconemella* represents a monophyletic lineage, clearly distinct from other genera within the family Criconematidae (Nguyen et al. 2022; Archidona-Yuste et al. 2024; Peraza-Padilla et al. 2025). This finding is also consistent with recent studies indicating that global biodiversity within *Xenocriconemella* is significantly higher than previously recognised (Archidona-Yuste et al. 2024; Peraza-Padilla et al. 2024; Cantalapiedra-Navarrete et al. 2024; Peraza-Padilla et al. 2024).

Given the limited number of specimens and the restricted geographic scope of sampling, further investigations encompassing a wider range of regions and habitats across Iran are necessary to gain a comprehensive understanding of the true diversity and distribution of *Xenocriconemella* species. The present findings also underscore the importance of sustained nematode surveys in natural environments, which are crucial for uncovering hidden biodiversity that may be overlooked by traditional taxonomic approaches alone.

In conclusion, the integrative taxonomic approach employed in this study has proven essential for resolving the complex taxonomy of ring nematodes. The description of *Xenocriconemella persica* sp. nov. adds valuable data to our understanding of nematode biodiversity, both within Iran and on a global scale. This discovery offers important insights into the diversity of nematodes inhabiting natural ecosystems and underscores the significance of ongoing surveys in ecologically rich regions such as the Hyrcanian forests. Furthermore, the identification of *X. persica* sp. nov. raises the possibility that several populations currently attributed to broadly defined species, such as *X. macrodora*, may in fact represent cryptic taxa that warrant formal taxonomic and molecular re-evaluation.

Ethical standards

The result of this work has not been published previously and is not under consideration elsewhere.

Ethical approval

The conducted research is not either related to human or animals' use.

Conflict of interest

Authors stated no conflict of interest.

Acknowledgements

A. Archidona-Yuste is funded by the Ramón y Cajal program (RYC2021-031108-I), and Juan de la Cierva programs (JDC2022-048855-I) funded by MCIN/AEI/10.13039/501100011033 and UE "Next Generation EU/PRTR".

References

Altschul SF, Gish W, Miller W, Myers EW, Lipman DJ (1990) Basic local alignment search tool. Journal of Molecular Biology 215(3): 403–410. https://doi.org/10.1016/S0022-2836(05)80360-2

Archidona-Yuste A, Navas-Cortes JA, Cantalapiedra-Navarrete C, Palomares-Rius JE, Castillo P (2016) Cryptic diversity and species delimitation in the *Xiphinema americanum*-group complex (Nematoda, Longidoridae) as inferred from morphometrics and molecular markers. Zoological Journal of the Linnean Society 176(2): 231–265. https://doi.org/10.1111/zoj.12316

Archidona-Yuste A, Cai R, Cantalapiedra-Navarrete C, Carreira JA, Rey A, Viñegla B, Liébanas G, Palomares-Rius JE, Castillo P (2020) Morphostatic speciation within the dagger nematode *Xiphinema hispanum*-complex species (Nematoda, Longidoridae). Plants 9(12): 1649. https://doi.org/10.3390/plants9121649

Archidona-Yuste A, Palomares-Rius JE, Clavero-Camacho I, Cantalapiedra-Navarrete C, Liébanas G, Castillo P (2023) A blind-identification test on *Criconema annuliferum* (de Man, 1921) Micoletzky, 1925 species complex corroborate the hyper-cryptic species diversity using integrative taxonomy. Plants 12(5): 1044. https://doi.org/10.3390/plants12051044

Archidona-Yuste A, Clavero-Camacho I, Ruiz-Cuenca AN, Cantalapiedra-Navarrete C, Liébanas G, Castillo P, Palomares-Rius JE (2024) The more we search, the more we find: discovering and expanding the biodiversity in the ring nematode genus *Xenocriconemella* De Grisse & Loof, 1965 (Nematoda: Criconematidae). Zoological Letters 10(1): 8. https://doi.org/10.1186/s40851-024-00230-3

Cai R, Archidona-Yuste A, Cantalapiedra-Navarrete C, Palomares-Rius JE, Castillo P (2020) New evidence of cryptic speciation in the family Longidoridae (Nematod: Dorylaimida). Journal of Zoological Systematics and Evolutionary Research 58(4): 869–899. https://doi.org/10.1111/jzs.12393

Cantalapiedra-Navarrete C, Navas-Cortés JA, Liébanas G, Vovlas N, Subbotin S, Palomares-Rius JE, Castillo P (2013) Comparative molecular and morphological characterisations in the nematode genus *Rotylenchus*: *Rotylenchus paravitis* n. sp., an example of cryptic speciation. Zoologischer Anzeiger 252(2): 246–268. https://doi.org/10.1016/j.jcz.2012.08.002

Cantalapiedra-Navarrete C, Clavero-Camacho I, Criado-Navarro I, Salazar-García R, García-Velázquez A, Palomares-Rius JE, Castillo P, Archidona-Yuste A (2024) Another new ring nematode, *Xenocriconemella andreae* sp. nov. (Nematoda, Criconematidae), from the Iberian Peninsula. Zoosystematics and Evolution 100: 1175–1190. https://doi.org/10.3897/zse.100.129009

Clavero-Camacho I, Palomares-Rius JE, Cantalapiedra-Navarrete C, León-Ropero G, Martín-Barbarroja J, Archidona-Yuste A, Castillo P (2021) Integrative taxonomy reveals hidden cryptic diversity within pin nematodes of the genus *Paratylenchus* (Nematoda: Tylenchulidae). Plants 10(7): 1454. https://doi.org/10.3390/plants10071454

Darriba D, Taboada GL, Doallo R, Posada D (2012) jModelTest 2: More models, new heuristics and parallel computing. Nature Methods 9: 772. https://doi.org/10.1038/nmeth.2109

Dayrat B (2005) Towards integrative taxonomy. Biological Journal of the Linnean Society. Linnean Society of London 85: 407–417. https://doi.org/10.1111/j.1095-8312.2005.00503.x

De Grisse AT (1969) Redescription ou modifications de quelques techniques utilisées dans l'étude de nématodes phytoparasitaires. Mededelingen Rijksfaculteit Landbouwwetenschappen Gent 34: 315–359.

De Ley P, Félix MA, Frisse LM, Nadler SA, Sternberg PW, Thomas WK (1999) Molecular and morphological characterisation of two reproductively isolated species with mirror-image anatomy (Nematoda: Cephalobidae). Nematology 1: 591–612. https://doi.org/10.1163/156854199508559

Derycke S, Remerie T, Vierstraete A, Backeljau T, Vanfleteren J, Vincx M, Moens T (2005) Mitochondrial DNA variation and cryptic speciation within the free-living marine nematode *Pellioditis marina*. Marine Ecology Progress Series 300: 91–103. https://doi.org/10.3354/meps300091

Eskandari A (2018) Nematodes of the families Criconematidae and Hemicycliophoridae. In: Ghaderi R, Kashi L, Karegar A (Eds) Plant-parasitic nematodes in Iran. Science Reference in collaboration with the Iranian Society of Nematology, 113–192.

Eskandari A, Karegar A, Pourjam E, Alizadeh A (2006) Three new records of Criconematidae (Nematoda: Tylenchida) from Iran. Iranian Journal of Plant Pathology 42: 153–157.

Etongwe CM, Singh PR, Bert W, Subbotin SA (2020) Molecular characterisation of some plant-parasitic nematodes (Nematoda: Tylenchida) from Belgium. Russian Journal of Nematology 28: 1–28. https://doi.org/10.24411/0869-6918-2020-10001

Fišer C, Koselj K (2022) Coexisting Cryptic Species as a Model System in Integrative Taxonomy. In: Monro AK, Mayo SJ (Eds) Cryptic Species: Morphological Stasis, Circumscription, and Hidden Diversity. Systematics Association Special Volume Series. Cambridge University Press, 169–196. https://doi.org/10.1017/9781009070553.007

Ghaderi R, Kashi L, Karegar A (2012) Species of the superfamily Criconematoidea (Nematoda: Tylenchomorpha) in Iran. 20th Iranian Plant Protection Congress, IRIPP, Shiraz.

Hall TA (1999) BioEdit: A user-friendly biological sequence alignment editor and analysis program for windows 95/98/NT. Nucleic Acids Symposium Series 41: 95–98.

Hamilton CA, Hendrixson BE, Brewer MS, Bond JE (2014) An evaluation of sampling effects on multiple DNA barcoding methods leads to an integrative approach for delimiting species: A case study of the North American tarantula genus *Aphonopelma* (Araneae, Mygalomorphae, Theraphosidae). Molecular Phylogenetics and Evolution 71: 79–93. https://doi.org/10.1016/j. ympev.2013.11.007

Holterman M, Van Der Wurff A, van Den Elsen S, van Megen H, Bongers T, Holovachov O, Bakker J, Helder J (2006) Phylum-wide analysis of SSU rDNA reveals deep phylogenetic relationships among nematodes and accelerated evolution toward crown clades. Molecular Phylogenetics and Evolution 23(9): 1792–1800. https://doi.org/10.1093/molbev/msl044

Hu M, Chilton NB, Gasser RB (2002) Single-stranded conformation polymorphism-based analysis of mitochondrial cytochrome c oxidase subunit 1 reveals significant substructuring in hookworm populations. Electrophoresis 23(1): 27–34. https://doi.org/10.1002/1522-2683(200201)23:1<27:AID-ELPS27>3.0.CO;2-7

Jenkins WR (1964) A rapid centrifugal-flotation technique for separating nematodes from soil. The Plant Disease Reporter 48: 692.

Katoh K, Rozewicki J, Yamada KD (2019) MAFFT online service: Multiple sequence alignment, interactive sequence choice and visualization. Briefings in Bioinformatics 20: 1160–1166. https://doi.org/10.1093/bib/bbx108

Le S, Josse J, Husson F (2008) FactoMineR: An R Package for Multivariate Analysis. Journal of Statistical Software 25: 1–18. https://doi.org/10.18637/jss.v025.i01

Masters BC, Fan V, Ross HA (2011) Species delimitation a Geneious plugin for the exploration of species boundaries. Molecular Ecology Resources 11(1): 154–157. https://doi.org/10.1111/j.1755-0998.2010.02896.x

Montgomery DC, Peck EA, Vining GG (2012) Introduction to Linear Regression Analysis. Wiley, New York.

Nguyen HT, Nguyen TD, Le TML, Trinh QP, Bert W (2022) Remarks on phylogeny and molecular variations of criconematid species (Nematoda: Criconematidae) with case studies from Vietnam. Scientific Reports 12: 14832. https://doi.org/10.1038/s41598-022-18004-2

Niasti F, Eskandari A, Maafi ZT, Saeedizadeh A (2016) Four known species of plant-parasitic nematodes of the genera *Crossonema* Mehta & Raski, 1971 and *Ogma* Southern, 1914 in Ramsar forests, northern Iran. Iranian Journal of Plant Pathology 52: 357–373.

Peraza-Padilla W, Aráuz-Badilla J, Cantalapiedra-Navarrete C, Palomares-Rius JE, Archidona-Yuste A, Castillo P (2024) A new ring nematode, *Xenocriconemella costaricense* sp. nov., (Nematoda: Criconematidae) from Costa Rica. Journal of Helminthology 98: e39. https://doi.org/10.1017/S0022149X24000294

Peraza-Padilla W, Artavia-Carmona R, Aráuz-Badilla J, Liébanas G, Cantalapiedra-Navarrete C, Salazar-García R, García-Velázquez A, Palomares-Rius JE, Castillo P, Archidona-Yuste A (2025) New insights into the phylogeny and morphometry of ring nematodes of the subfamily Discocriconemellinae (Nematoda: Criconematidae): *Xenocriconemella* and *Discocriconemella*. Zoological Journal Linnean Society of London. https://doi.org/10.1093/zoolinnean/zlaf111

Powers TO, Harris TS, Higgins RS, Mullin PG, Powers KS (2021) Nematode biodiversity assessments need vouchered databases: A BOLD reference library for plant-parasitic nematodes in the superfamily Criconematoidea. Genome 64: 232–241. https://doi.org/10.1139/gen-2019-0196

Proudlove G, Wood PJ (2003) The blind leading the blind: Cryptic subterranean species and DNA taxonomy. Trends in Ecology & Evolution 18: 272–273. https://doi.org/10.1016/S0169-5347(03)00095-8

R Core Team (2022) R: a language and environment for statistical computing. R Foundation for Statistical Computing, Vienna, Austria. https://www.R-project.org/

Rambaut A (2018) FigTree v1.4.4, A graphical viewer of phylogenetic trees. http://tree.bio.ed.ac.uk/software/figtree/

Ronquist F, Huelsenbeck JP (2003) MRBAYES 3: Bayesian phylogenetic inference under mixed models. Bioinformatics (Oxford, England) 19: 1572–1574. https://doi.org/10.1093/bioinformatics/btg180

Rosenberg NA (2007) Statistical tests for taxonomic distinctiveness from observations of monophyly. Evolution; International Journal of Organic Evolution 61: 317–323. https://doi.org/10.1111/j.1558-5646.2007.00023.x

Ross HA, Murugan S, Li WL (2008) Testing the reliability of genetic methods of species identification via simulation. Systematic Biology 57(2): 216–230. https://doi.org/10.1080/10635150802032990

Seinhorst JW (1966) Killing nematodes for taxonomic study with hot F.A. 4:1. Nematologica 12: 178. https://doi.org/10.1163/187529266X00239

Subbotin SA, Vierstraete A, De Ley P, Rowe J, Waeyenberge L, Moens M, Vanfleteren JR (2001) Phylogenetic relationships within the cyst-forming nematodes (Nematoda, Heteroderidae) based on analysis of sequences from the ITS regions of ribosomal DNA. Molecular Phylogenetics and Evolution 21: 1–16. https://doi.org/10.1006/mpev.2001.0998

Subbotin SA, Vovlas N, Crozzoli R, Sturhan D, Lamberti F, Moens M, Baldwin J (2005) Phylogeny of Criconematina Siddiqi, 1980 (Nematoda: Tylenchida) based on morphology and D2-D3 expansion segments of the 28S-rRNA gene sequences with application of a secondary structure model. Nematology 7: 927–944. https://doi.org/10.1163/156854105776186307

Tan G, Muffato M, Ledergerber C, Herrero J, Goldman N, Gil M, Dessimoz C (2015) Current methods for automated filtering of multiple sequence alignments frequently worsen single-gene phylogenetic inference. Systematic Biology 64(5): 778–791. https://doi.org/10.1093/sysbio/syv033

Taylor AL (1936) The genera and species of the Criconematinae, a subfamily of the Anguillulinidae (Nematoda). Transactions of the American Microscopical Society 55(4): 391–421. https://doi.org/10.2307/3222522

Zaker Abbasali S, Sahebani N, Jahanshahi Afshar F, Karimi S (2024) Report of nine species of Criconematidae nematodes from forests of the Mazandaran Province. Iranian Plant Pathology Science 13: 1–13. https://doi.org/10.61186/pps.13.2.1